Mercury distribution, partitioning and speciation in coastal vs. inland High Arctic snow

Alexandre J.Poulain, Edenise Garcia, Marc Amyot, Peter G.C. Campbell, Parisa A. Ariya

Abstract

Atmospheric mercury deposition on snow at springtime has been reported in polar regions, potentially posing a threat to coastal and inland ecosystems receiving meltwaters. However, the post-depositional fate of Hg in snow is not well known, and no data are available on Hg partitioning in polar snow. During snowmelt, we conducted a survey of Hg concentrations, partitioning and speciation in surface snow and at depth, over sea ice and over land along a 100 km transect across Cornwallis Island, NU, Canada. Total Hg concentrations [THg] in surface snow were low (less than 20 pmol L^{-1}) and were significantly higher in marine vs. inland environments. Particulate Hg in surface snow represented up to 90% of total Hg over sea ice and up to 59% over land. At depth, [THg] at the snow/sea ice interface (up to 300 pmol L^{-1}) were two orders of magnitude higher than at the snow/lake ice interface (ca. 2.5 pmol L^{-1}). Integrated snow columns, sampled over sea-ice and over land, showed that particulate Hg was mostly bound to particles ranging from 0.45 to 2.7 μm. Moreover, melting snowpacks over sea ice and over lake ice contribute to increase [THg] at the water/ice interfaces. This study indicates that, at the onset of snowmelt, most of the Hg in snow is in particulate form, particularly over sea ice. Low Hg levels in surface snow suggest that Hg deposited through early spring deposition events is partly lost to the atmosphere from the snowpack before snowmelt. The sea ice/snow interface may constitute a site for Hg accumulation, however. Further understanding of the cycling of mercury at the sea ice/snow and sea ice/seawater interfaces is thus warranted to fully understand how mercury enters the arctic food webs.

1. Introduction

The discovery of mercury depletion events in the high Arctic (Schroeder et al., 1998, Lu et al., 2001, Lindberg et al., 2002, Steffen et al., 2002), Antarctic (Ebinghaus et al., 2002) and in sub-Arctic areas (Dommergue et al., 2003b, Poissant and Pilote, 2003), resulting in rapid, near complete depletion of Hg from the atmosphere, provides evidence that atmospheric oxidation of Hg is faster than initially proposed (Swain et al., 1992). These oxidation processes are thought to occur in marine environments (Sprovieri et al., 2005), and to involve reactive halogen radicals from sea-salt aerosols (Lindberg et al., 2002). Recent studies showed that Br and BrO radicals were the most effective halogens driving gaseous elemental mercury oxidation (Ariya et al., 2002). Together, modeling studies of atmospheric transport of Hg originating from Asia, Europe and to a lesser extent, North America, to higher latitudes combined with the rapid depletion of gaseous elemental mercury suggest that the Arctic is a sink for Hg (Ariya et al., 2004). The main products of Mercury Depletion Events are reactive gaseous species and particulate-phase Hg (Schroeder et al., 1998, Lu and Schroeder, 2004).

Gauchard et al. (2005) observed an increase in particles larger than 0.3 μm in ambient air during an atmospheric depletion event, as well as a subsequent redistribution of the atmospheric particulate fraction to bigger sizes after the event ended. The same study suggested that particles of a size comprised between 0.5 and 5 μm were more likely to be associated with mercury depletion events than the smaller ones. These atmospheric processes may affect the partitioning of Hg in underlying snow, hence the need to better assess Hg association with particles in snow.

The pool of Hg in surface snow, although periodically and dramatically enriched during mercury depletion events (Lu et al., 2001), decreases at the onset of snowmelt, and can reach low levels that are comparable to what can be found in pristine environments (Lindberg et al., 2002, Steffen et al., 2002, Poulain et al., 2004, St Louis et al., 2005). This decrease in total Hg concentrations in the snowpack is likely related to the photoreduction of Hg(II) and its subsequent evasion to the atmosphere (Lalonde et al., 2002, Lalonde et al., 2003) or to a loss associated with snowmelt water during early melt episodes (Steffen et al., 2002, Dommergue et al., 2003a). Recent work showed that Hg concentrations in direct proximity to sea ice leads could reach unprecedented levels of *ca.* 4 nmol L^{-1} (Douglas et al., 2005). These data, together with laboratory studies that underscored that bromine-derived reactive compounds originating from sea-salt aerosols were involved in fast oxidation of atmospheric Hg (Ariya et al., 2002), suggest that Hg cycling in coastal/marine environments is highly dynamic, possibly leading to Hg accumulation in these areas (Douglas and Sturm, 2004). There is, therefore, a need to better characterize the behaviour of Hg in snow at the interface between marine and inland systems. In particular, there is very limited information available on the partitioning of Hg in marine and inland polar snow.

The purpose of this paper is to establish the distribution, partitioning and speciation of total Hg (THg) in surface snow deposited over land and over sea ice along a 100 km transect encompassing two coastal areas. The role of snow/ice interfaces as potential accumulation areas for Hg over sea and lake waters was also investigated.

2. Methods

2.1. Sampling protocol and locations

To establish the spatial distribution and speciation of total Hg from marine to inland snow, surface snow was sampled along a transect NW–SE across Cornwallis island, NU, Canada (Fig. 1a) on 17 June 2004. Sampling started over the sea-ice between Little Cornwallis and Cornwallis islands and extended to the sea-ice between Cornwallis and Devon islands for a total of 11 sites (Fig. 1b; surface snow physical properties at the 11 transect sampling sites are given in Table 1). Sampling for depth profiles and particulate distribution took place in the south-west part of Cornwallis Island (Fig. 1b). Sampling was undertaken when average daily air temperatures started to exceed the freezing point as recorded by Environment Canada at the Resolute Bay station (Fig. 2a and b) and when snow was starting to melt. Note that for each site and snow stratum sampled, temperature was recorded to better assess snow properties.

2.1.1. Transect surface snow sampling

Transect sampling was carried out on 7 June 2004. Snow sampling was done by collecting triplicate snow samples from the first centimetre of the surface of the snowpack by filling 1 L fluorinated ethylene propylene copolymer (Teflon FEP) bottles, using a Teflon shovel. All containers used for Hg sampling and analysis were previously acid-washed and thoroughly rinsed with milliQ water (R > 18.2 MΩ cm). Clean hands/dirty hands techniques were used, and integral Tyvek® body suits and non-powdered gloves were worn at all times in order to avoid contamination.

2.1.2. Snow depth profiles

Snow accumulation over sea ice and over land was sampled on 9 June 2004. For snow depth profiles, triplicate samples were taken from each snow stratum. One replicate corresponded to one litre of snow collected in a Teflon bottle using a Teflon shovel. Three snow strata were sampled over sea ice and four snow strata were sampled over lake ice. Snow strata were determined by the state of metamorphism of the snow grains, as defined in the international classification of seasonal snow on the ground (Colbeck et al., 1985). Snow grain identification and size determination was carried out in the field, using a binocular over a black, cold (T < 0 °C), background. Snow density as well as the temperature of the layer at mid depth were also measured. Snow for cation analyses was collected in 30 mL high density polyethylene (HDPE) Nalgene bottles that had previously been thoroughly cleaned, rinsed with ultrapure water and acidified to 0.1% with HCl (64%, Omnitrace grade). Snow for anion analyses was collected in 30 mL HDPE Nalgene

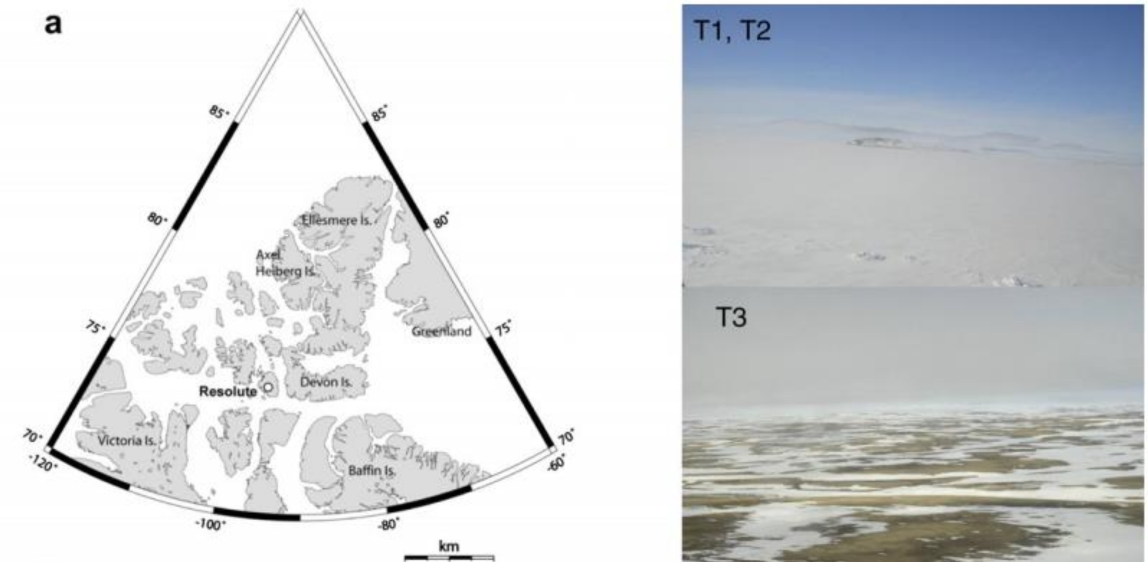

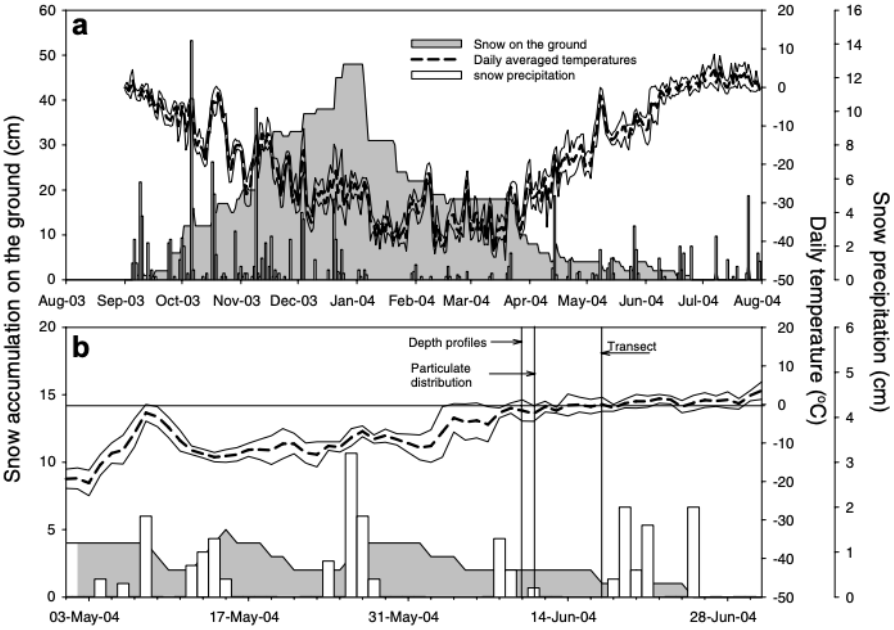

Fig. 2. Meteorological data from the met site in Resolute Bay. (a) From September 2003 to September 2004 and (b) from May 2004 to July 2004. Snow accumulation on the ground at the met site, snow precipitation, and daily average temperature are presented. Note that the upper and lower continuous black lines represent maximum and minimum daily temperatures.

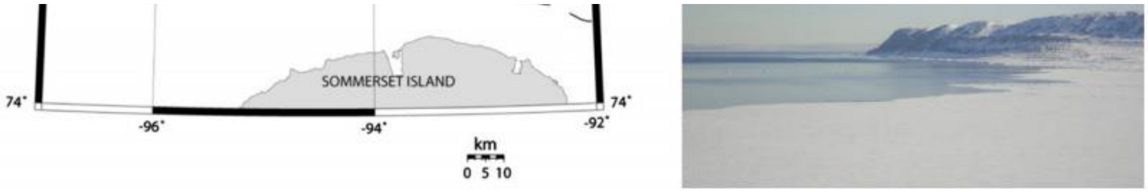

Fig. 1. (a) Location of Cornwallis Island in the Canadian High Arctic. (b) Location of sampling sites during the transect survey. Pictures on the right-hand side refer to the transect. Note that the white triangle at the bottom right of the graph refers to an open water area (no ice present), as depicted in picture T9, T10, T11. Maps were designed from http://www.aquarius.geomar.de/omc/omc_project.html#PSP.

Table 1
Surface snow physical properties at the 11 sampling sites of the transect

	Site	Altitude (m; a.s.l.)	Snow density %	Temp. surface (°C)	Temp. bottom (°C)	Snow depth (cm)	Symbol	Grain size (mm)
T1	Sea ice	0	40	0.5	0	9	⌂	2–4
T2	Sea ice	0	48	0.5	0	20	∵	2–4
T3	Coastal area	10	42	0	−0.5	40	⌂	2–4
T4	Inland	178	36	0	−5	46	⌂	2
T5	Inland	169	34	−0.5	−9	41	⌂	1–5
T6	Inland	236	28	0	−10	36	⌂	1–2
T7	Inland	289	42	−0.5	−5	20	∵	2.4
T8	Inland	220	55	0.5	0	55	∵	3–4
T9	Coastal area	179	50	0	−4	20	∵	2–3
T10	Sea ice	0	48	0	0.5	12	⌂	2–4
T11	Sea ice	0	42	0	−1	9	⌂	2–4

⌂ represents mixed formed crystals (faceted crystals with potentially recent rounding due to decrease in temperature gradient) and ∵ represent melt clusters.

bottles, previously thoroughly rinsed with ultrapure water. All samples were kept in the dark and at 4 °C until they were analysed. Note that due to the rapid melt occurring at this time and considering the time required to carry out all the analyses within a few hours of sampling, each site was sampled over depth only once during this period.

2.1.3. Lake/seawater depth profiles

Water was pumped from the depth of interest using a neoprene-coated Teflon line and a peristaltic pump (Masterflex™). The neoprene coating protected the water circulating in the tubing from exposure to solar radiation. Prior to deployment in the field, the line was thoroughly washed with HCl 20% (v/v) by continuously circulating the acidic solution through the line for 30 min. The line was then carefully rinsed with ultrapure water; achievement of proper rinsing of the line was monitored by measuring the conductivity of the circulating solution and rinsing stopped when the solution reached levels below 3 μS cm^{-1}, corresponding to that of ultrapure water. In the field, the line was rinsed with the water at each depth of interest prior to taking samples from that depth. Acid-washed Teflon bottles were rinsed with the water from the depth of interest four times prior to the actual sampling; samples were taken in triplicate.

2.2. Chemical analysis and bacterial counts

Total Hg concentrations in snow were quantified with the method described by Lalonde et al. (2003) and based on Gill and Bruland (1990), using a mercury fluorescence detector (Tekran™ Model 2500). Briefly, Hg in water samples was reduced using 1% $NaBH_4$ (w/v) and 4 M NaOH. Approximately 100 mL of water or melted snow was poured into a 250 mL glass bubbler and purged for 15 min with clean air from a Hg-free air generator (Tekran™ Model 1100) additionally stripped of Hg(0) by passage over a gold filter at a flow rate of ca. 1 L min^{-1}. The working detection limit of this method, calculated in the field, was 0.45 pmol L^{-1} or three times the standard deviation of ten procedural blanks. Triplicates were systematically taken and typically varied between 0.5% and 10%. Average blank values were below the detection limit.

Anions were analyzed by ion chromatography using a DIONEX ICS 2000. A 25-μL sample of melted snow was introduced into the injection loop and separation occurred through an AS-17 column topped with a AG-17 pre-column. The elution step involved the passage of a KOH solution with a concentration gradient from 15 to 30 mmol L^{-1}. Cations were analysed with an inductively coupled plasma atomic emission spectrometer (ICP-AES Vista AX) using an internal standard of Yttrium (5 mg L^{-1}). With this method variability was within 5%. For very few high salinity samples, deviation from the expected control value reached up to 39%. In these latter cases, samples were diluted and reanalysed to achieve proper replicability.

2.3. Modeling of the dissolved inorganic speciation of Hg

To assess the inorganic speciation of Hg in melted snow and water, a chemical equilibrium program was used (MINEQL+, version 4.5) (Schecher and McAvoy, 1992). Cations and metals entered in the model were calcium, iron, magnesium, mercury, potassium and sodium. Anions used were bromide, chloride, nitrate and sulphate as well as hydroxide derived from the pH of the sample. The solutions were considered to be in equilibrium with the atmosphere and carbonate species were estimated by the model using the pH of the samples. Data were corrected for the ionic strength of the sample; ionic strength was calculated by the model with the Davies equation. Stability constants used in the model are presented in Table 2. The complexation of Hg with dissolved organic matter (DOM) is not presented due to the current lack of consensus regarding binding constants for Hg-DOM complexation reactions. However, the model included small organics such as acetate and formate usually found in Arctic snow (Toom-Sauntry and Barrie, 2002). Hg complexation, whether it is inorganic or organic, is strongly influenced by the pH of the solution. Several studies have shown that the pH of a solution may change upon the dissolution of acidic aerosols (Riordan et al., 2005), likely to be the case during snowmelt. While speciation results presented in this paper were based on the measured pH of melted snow, sensitivity tests were performed for snow samples in which the model was run over a pH range of ±1 pH unit above and below the measured pH value. Moreover, to take into consideration uncertainties inherent in the estimation of the complexation constants, the model was ran with binding constants ±1 order of magnitude. Results showed shifts in the relative importance of the species, altogether with differences ranging from 4% to 40% from the initial values, but these variations did not affect the conclusions presented in the paper.

Table 2
Reactions and stability constants used in the model MINEQL+ ver. 4.5

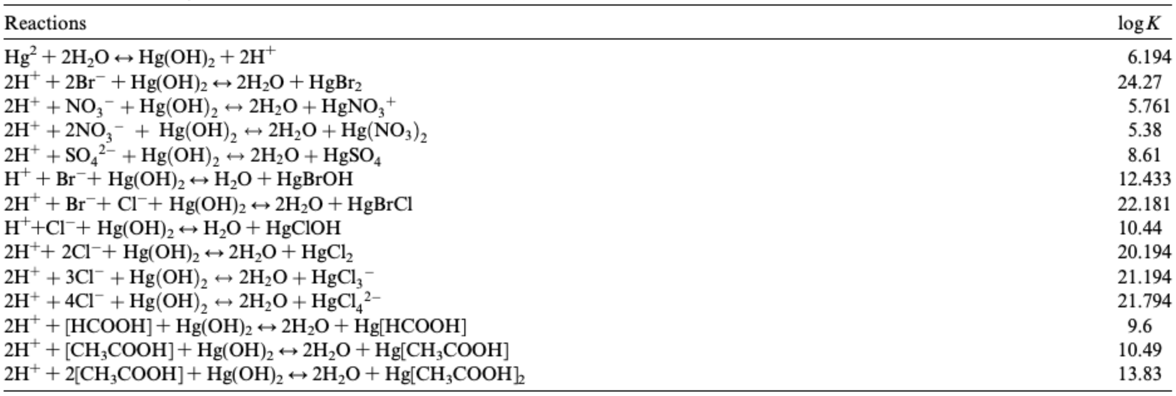

Reactions	log *K*
$Hg^2 + 2H_2O \leftrightarrow Hg(OH)_2 + 2H^+$	6.194
$2H^+ + 2Br^- + Hg(OH)_2 \leftrightarrow 2H_2O + HgBr_2$	24.27
$2H^+ + NO_3^- + Hg(OH)_2 \leftrightarrow 2H_2O + HgNO_3^+$	5.761
$2H^+ + 2NO_3^- + Hg(OH)_2 \leftrightarrow 2H_2O + Hg(NO_3)_2$	5.38
$2H^+ + SO_4^{2-} + Hg(OH)_2 \leftrightarrow 2H_2O + HgSO_4$	8.61
$H^+ + Br^- + Hg(OH)_2 \leftrightarrow H_2O + HgBrOH$	12.433
$2H^+ + Br^- + Cl^- + Hg(OH)_2 \leftrightarrow 2H_2O + HgBrCl$	22.181
$H^+ + Cl^- + Hg(OH)_2 \leftrightarrow H_2O + HgClOH$	10.44
$2H^+ + 2Cl^- + Hg(OH)_2 \leftrightarrow 2H_2O + HgCl_2$	20.194
$2H^+ + 3Cl^- + Hg(OH)_2 \leftrightarrow 2H_2O + HgCl_3^-$	21.194
$2H^+ + 4Cl^- + Hg(OH)_2 \leftrightarrow 2H_2O + HgCl_4^{2-}$	21.794
$2H^+ + [HCOOH] + Hg(OH)_2 \leftrightarrow 2H_2O + Hg[HCOOH]$	9.6
$2H^+ + [CH_3COOH] + Hg(OH)_2 \leftrightarrow 2H_2O + Hg[CH_3COOH]$	10.49
$2H^+ + 2[CH_3COOH] + Hg(OH)_2 \leftrightarrow 2H_2O + Hg[CH_3COOH]_2$	13.83

The log *K* values used in the MINEQL+ simulations were taken from "Critical Selected Stability Constant of Metal Complexes", National Institute of Standards and Technology (NIST) Standard Reference Database.

2.4. Partitioning of Hg onto particles and elemental composition of particles

2.4.1. Partitioning experiments

To identify to which size fraction particulate Hg was bound, one integrated snow column (*ca.* 20 L) was collected inland, and one over the sea-ice, on 13 June 2004, in a Tedlar® (polyvinyl fluoride) bag, previously acid washed and rinsed with ultrapure water. After a complete thaw was reached at room temperature, triplicate water samples from each bag were filtered through filters of decreasing porosities: 10 µm (polycarbonate), 2.7 µm (GF/B), 0.7 µm (GF/F), 0.45 µm (Gelman) and 0.2 µm (polycarbonate). The particulate Hg distribution was obtained by subtracting the Hg burden between two filters of consecutive pore sizes. To test for possible adsorption of Hg onto different filters, 125 mL of a standard solution freshly prepared in ultra-pure water (final concentration 10.22 ± 0.35 pmol L^{-1}, $n = 4$) was filtered through polycarbonate (0.2 µm, $n = 4$), Gelman (0.45 µm, $n = 3$) and glass fibre (0.7 µm, $n = 3$) filters. The volume of the standard that was filtered corresponded to the volume of the samples filtered, i.e. 125 mL. No significant difference was found between the control and the filtrates from glass fibre filters and Gelman filters. Filtrates from polycarbonate filters yielded values significantly lower than the control by 20% (*t*-test, $t = 7.08$, $p = 0.002$). Results presented in this paper were therefore corrected for this adsorption when polycarbonate filters were used. This method was compared to that of Sarica et al. (2004) which uses a direct mercury analyser and determines Hg content by pyrolysis of the filter; no statistical difference was found using either the subtraction method, presented here, or the pyrolysis method (Wilcoxon, $p = 0.334$). For bacterial counts, Falcon tubes were filled with snow, thawed at 4 °C and preserved with glutaraldehyde to a final concentration of 2%. Bacterial counts were determined using a flow cytometer following the protocol described in Gasol and Del Giorgio (2000).

2.4.2. Elemental composition of particles

In order to assess the elemental composition of the particles present in snow, a scanning electron microscope (Hitachi S-3000N Variable Pressure) coupled to an X-ray diffraction (XRD) probe, was used. Melted snow samples, from an integrated snow column, were filtered through glass fibre filters of a nominal porosity of 0.7 µm. Samples included snow collected inland ($n = 3$) and over the sea-ice ($n = 3$). Each filter was freeze-dried and cut to a size of 1 cm^2 in order to be put on an aluminium sample-holder. Prior to microscopic observation and elemental composition determination, filters were coated with an Au–Pd amalgam. Depending on the number of particles in the filters, a minimum of 10 and a maximum of 20 observations were made on each filter. In the microscope field of observation, depending on the magnification used, 5–20 particles were present. These particles were targeted for XRD analysis. Note that this technique allowed us to qualitatively determine the elemental inorganic composition; no quantitative analyses were performed on the filters.

2.5. Statistical analyses

Statistical analyses (correlations, regressions and comparisons of variances) were performed using JMP 4.1 (SAS). When data did not meet a normality and homoscedasticity, a non-parametric test was used to compare variances (Kruskal–Wallis). To comply with the normality criterion some data were log transformed. The level of significance for both parametric and non-parametric tests was 0.05.

3. Results

3.1. Distribution of total mercury in snow along a transect and with depth, inland and over sea ice

3.1.1. THg concentrations in surface snow along a transect

Total Hg concentrations ([THg]) were significantly higher in surface snow collected over the sea ice (10.2 ± 3.5 pmol L^{-1}, $n = 12$) than in surface snow collected over land (4.1 ± 3.5 pmol L^{-1}, $n = 21$) (Kruskal–Wallis test, $p = 0.037$) (Fig. 3a). However, no significant differences were observed (Kruskal–Wallis test, $p = 0.72$) in dissolved Hg concentrations (fraction less than 0.2 µm) from snow collected over sea ice or over land. Snow collected over sea-ice was enriched with chloride ions (0.20 ± 0.14 mmol L^{-1}, $n = 4$) compared to inland snow (0.01 ± 0.003 mmol L^{-1}, $n = 7$) (Fig. 3b). The proportion of Hg bound to particles was significantly higher (t-test, $t = -2.92$, $p = 0.016$) in snow collected over the sea-ice (79 ± 9%) than in snow collected over land (58 ± 16%). In the middle of Cornwallis Island, at site T6 (Fig. 3a), the Hg level (10.6 ± 5.7 pmol L^{-1}, $n = 3$) was higher than at other inland sites (3.0 ± 1.2 pmol L^{-1}, $n = 18$). Note that a heavy fog was present during sampling at this site (Fig. 1, picture T6). This peak in [THg] corresponded to a maximum in nitrate concentrations (94 µmol L^{-1}) (Fig. 3b), reflecting a significant but weak covariance observed between nitrate and particulate Hg across island samples ($r = 0.67$, $p = 0.024$, $n = 11$).

3.1.2. THg concentrations at depth within a snow accumulation

In order to compare Hg distribution at various depths within a snow column, two snow packs were sampled, (i) over sea ice and (ii) inland, over a frozen lake, in the south-western part of Cornwallis Island (see Fig. 1b for location, IS for inland site and MS for marine site). Clustered rounded crystals were observed over the frozen lake, indicating signs of snowmelt. Over sea ice, rounded crystals were present in the middle stratum as well as ice lenses in the center of the accumulation, indicating here again some signs of melt. Similar to results showing higher surficial [THg] in snow over sea ice, [THg] at depth within the snow columns were also higher over sea ice and showed a higher association with particles of a size greater than 0.2 µm; from 60% to 83% and from 21% to 53% of the Hg was bound to particles over sea ice and over land, respectively (Figs. 3a and 4c). These differences between coastal and inland snow were most striking at the snow/ice interface with [THg] two orders of magnitude higher in the coastal snow pack (Fig. 4a). In snow collected over sea-ice, [THg] was related to bromide ($r^2 = 0.99$, $p = 0.01$) and chloride ($r^2 = 0.99$, $p = 0.028$) concentrations. In snow collected inland, however, no relation was observed with chloride, and bromide ions were not detected. It should be noted, however, that the absence of a relationship in the latter case may be related to the smaller range of [Cl$^-$] observed within the inland snowpack (6.1×10^{-3} to 4.1×10^{-2} mmol L^{-1}), compared to the range observed over the sea-ice (0.26–163 mmol L^{-1}).

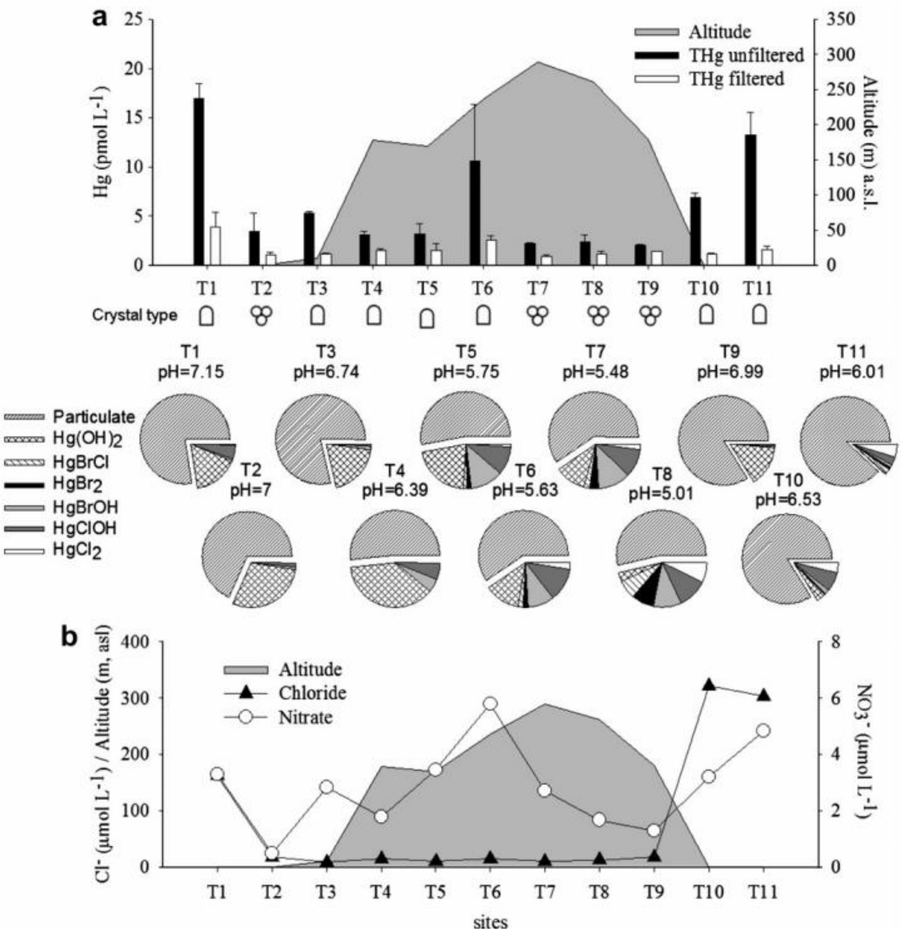

Fig. 3. (a) Total Hg concentrations (black bars) and dissolved Hg concentrations (white bars) over a transect, comprising 11 sites, across Cornwallis Island. Pies underneath each set of bars represent the particulate and dissolved inorganic speciation of Hg. (b) Chloride and nitrate concentrations for each of the 11 sites. ∩ represents mixed formed crystals (faceted crystals with potentially recent rounding due to decrease in temperature gradient) and ☘ represents melt clusters.

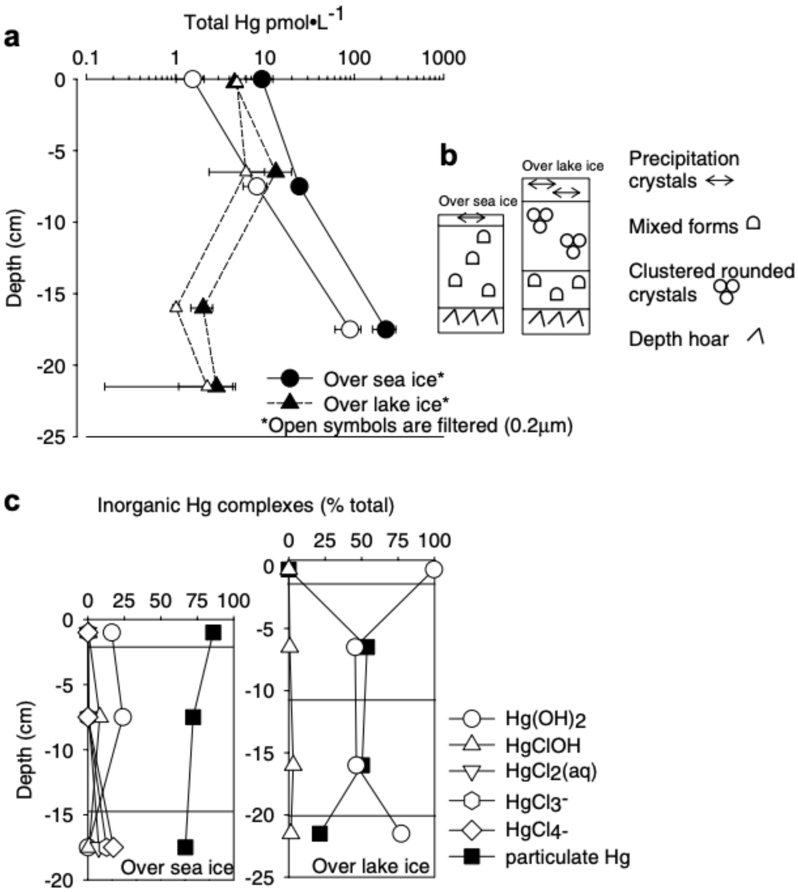

Fig. 4. (a) Depth profile of total mercury over sea ice (circle) and over land (triangles) in unfiltered (closed symbols) and filtered (open symbols) samples. (b) Snow stratigraphy at both sites. (c) Inorganic speciation of dissolved Hg.

3.2. Inorganic speciation of Hg in snow and partitioning onto particles

3.2.1. Inorganic speciation

The inorganic speciation of the dissolved fraction varied as a function of snow pH and halide concentrations. At the marine site, where salinity increased with depth, the dissolved phase was dominantly comprised of uncharged complexes at the surface and negatively charged chloro-complexes at depth (HgCl3- and HgCl42-) (Fig. 4c). Inland, particulate and dissolved phases were alternately dominant within the profile. The dissolved phase was mainly formed of $Hg(OH)_2$ with some contributions from mixed complexes such as HgClOH (Fig. 4c). To test for the effect on Hg speciation of low molecular weight organic molecules present in snow, such as formate and acetate, previously published concentrations recorded at Alert (NU, Canada) (Toom-Sauntry and Barrie, 2002) were used in the model. Even considering the maximum concentrations recorded for acetate and formate, our results show that inorganic complexes of Hg with OH, Cl^- and Br^- still dominated the speciation. Similar observations have been reported for snow collected at lower latitudes in the French Alps (Ferrari et al., 2002).

3.2.2. Hg partitioning onto particles

No Hg was detected adsorbed to particles of a nominal size greater than 10 µm or smaller than 0.2 µm, both in snow collected over land and in snow collected over sea ice (Fig. 5a and b). Most of the particulate Hg was bound to particles ranging from 2.7 to 10 µm in snow collected over land (62 ± 23%) and over sea-ice (53 ± 6%) (Fig. 5a and b). In snow collected inland, the remaining particulate Hg was bound to particles of a size ranging from 0.7 to 2.7 µm (12 ± 11%) and from 0.45 to 0.7 µm (20 ± 7%) (Fig. 5a). In snow collected over sea ice, the remaining particulate pool was significantly ($p = 0.004$, $n = 15$) more associated with the fraction [0.7–2.7 µm] (32 ± 4%) than with the fraction [0.45–0.7 µm] (17 ± 1%) (Fig. 5b). Snow was melted prior to the partitioning experiment. Hence, this experiment only reflects the association of Hg with insoluble or poorly soluble particles.

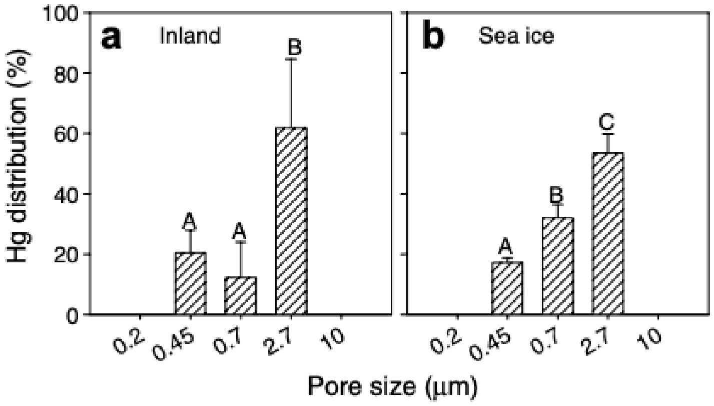

Fig. 5. Relative distribution of particulate Hg species in snow collected inland and over the sea-ice as a function of particle size. Different letters represent significant differences.

3.2.3. Elemental composition of particles

Elements present in the particles in snow included Al, Br, Ca, Fe, K, Na, O and Si. In most cases Si and Al were associated with the same particle, as were O, Mg and Ca, and Fe and O, suggesting the presence of sand grains (aluminosilicates), calcium carbonates and iron oxides. This interpretation was confirmed by visual observations, e.g. in the case of the cubic arrangement of calcium carbonate deposits. Since glass fibre filters were used, the presence of Si might be partly due to contamination from the filter. Note that with this technique one could not assess the composition of organics and soluble aerosols since snow was thawed, and high energy SEM is not adequate for detailed organic analysis.

3.3. THg concentrations in lake water and seawater underlying a snow accumulation

In order to assess the impact of the snowpack on underlying waters, the whole lake water column was sampled, from the surface to a depth of 10 m and the first 11.5 m of the sea water column. At both sites, [THg] concentrations were highest at the surface, between ice edges, and subsequently decreased three- to fourfold and stayed fairly stable in the remainder of the sampled zone (Fig. 6a and b). For all the other elements analysed, concentrations increased or remained stable from the surface to a depth of 11.5 m (Table 4, Fig. 6b). In seawater, the fraction of Hg bound to particles greater than 0.45 μm in the upper part of the lead was ca. 45% and only 15% and 6% at 5.5 m and 11.5 m, respectively, indicating a greater importance of particulate Hg forms at the surface in direct proximity to the snowpack (Fig. 6b).

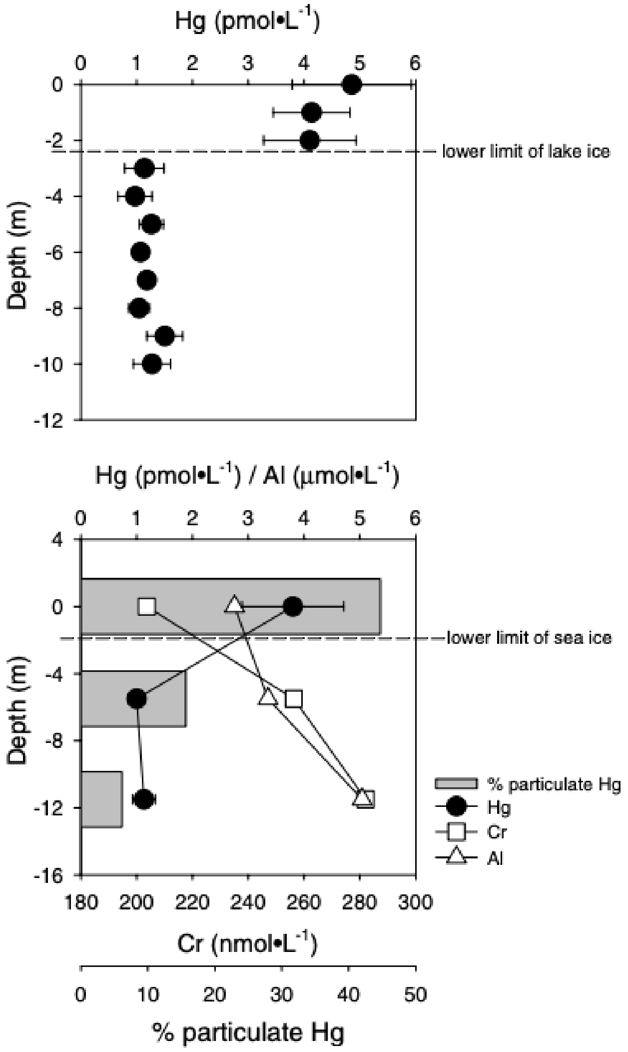

Fig. 6. Depth profile of total mercury concentrations within the water column of ice-covered North lake (a) and depth profile of total mercury concentrations, down to 11.5 m, in Barrow Strait, between Cornwallis and Griffith Islands (b). Samples were collected through a 10 cm wide crack in sea ice.

Based on snow thickness and snow density for each stratum, the estimated pool of Hg stored in snow over sea ice and over lake ice was ca. 4500 pmol m^{-2} and 850 pmol m^{-2}, respectively. By comparing THg concentrations in water at depths below the ice (below 2 m), as a reference level for the pre-melt period, and THg concentrations measured at the surface, we calculate that ca. 500 and 100 pmol m^{-2} of Hg are required, over sea ice and over lake ice, respectively, to increase the concentrations from that of the pre-melt period to the levels observed at the time of sampling. These estimates suggest that melting of only 11% (over sea ice) or 14% (over lake ice) of the snowpack is required to result in these Hg levels.

4. Discussion

4.1. Concentrations and speciation of THg concentrations in surface snow along a transect over land and sea ice

[THg] as well as the proportion of particulate forms of Hg were consistently and significantly higher in snow collected over sea ice (up to 300 pmol L^{-1} and 68% to 88%, respectively) than in snow collected over land (up to 15 pmol L^{-1} and 31% to 59%, respectively) (Fig. 3, Fig. 4a and c). High concentrations of Hg were previously reported in Arctic snow samples and were associated with mercury depletion events, more likely to occur in systems under marine influence (Douglas et al., 2005). However, the concentrations reported here are lower than those observed in other locations in the Arctic (ca. 450 pmol L^{-1}: (Lu et al., 2001, Lindberg et al., 2002)). Indeed, our results were representative of samples collected during late spring (from 9 to 17 June), a period during which mercury depletion events were less likely to occur and associated with a decrease in the pool of THg because of the initiation of snowmelt (Lindberg et al., 2002, Ferrari et al., 2004). Note that Lalonde et al. (2001) and Lalonde et al. (2003) showed that chloride enhances Hg(0) oxidation in water and decreases Hg(II) reduction when added to snow. Hence, the higher total Hg concentrations in coastal/marine snow may reflect the damping effect of halides on the post-depositional redox cycling of Hg to the atmosphere. In the following Section 4.2. other mechanisms likely to be responsible for a loss of Hg from the snow surface are discussed.

The increase in [THg] in the middle of the island (Fig. 3a) was likely the result of deposition of atmospheric Hg associated with fog droplets (note that fog was only present at Site T6). In a recent study in the coastal area around the Bay of Fundy, eastern Canada, Ritchie et al. (2006) reported very high levels of Hg in fog (two orders of magnitude greater than what was observed in surface snow: up to 425 ng L^{-1} or ca., 2000 pmol L^{-1}). The highest levels reported by these authors were recorded at high altitudes in coastal areas. Hence, it is likely that fog can be a source of Hg to terrestrial ecosystems, as is the case for nutrients (e.g. NO3-)) (Weathers, 1999) and further investigation of its dynamics is warranted.

The particulate fraction of Hg found throughout Cornwallis Island, inland (up to 59%) as well as over sea-ice (up to 88%), was bound to particles within the 0.45 μm to 10 μm size class and especially to larger particles within this size range (2.7–10 μm) (Fig. 5a and b). These size fractions correspond to the accumulation and coarse modes defined for aerosols and which may be involved in Arctic Haze (Staebler et al., 1994) as well as to the particulate fraction associated with mercury depletion events (Gauchard et al., 2005). The accumulation mode includes particles from 0.1 to 1 μm produced mainly through coalescence of smaller particles; the coarse mode is mostly formed of sea-salt and soil particles (>1 μm) (Staebler et al., 1994). The presence of aluminosilicates, calcium carbonates and iron oxides as well as sodium confirms the terrigenous and marine origin of some particles. Since snow was thawed prior to the partitioning analysis, it is likely that some aerosols disappeared due to the phase change. Hence these observations are more representative of wet snow or snowmelt water rather than dry cold solid snow. It is therefore likely that the total concentrations of particulate Hg in solid snow, including water-soluble aerosols, are greater than the estimates reported here. To the best of our knowledge this is the first attempt to assess the post-depositional partitioning of Hg between dissolved and solid phases in arctic snow. Nevertheless, the increased proportion of particles in the range 0.7–2.7 μm over sea ice (ca. 30% Fig. 5b) compared to inland (ca. 10% Fig. 5a) may reflect the increased importance of sea salt aerosols deposited onto snow in marine environments (Vogt et al., 1996), which are likely to be involved in fast oxidation of elemental mercury (Lindberg et al., 2002).

A growing body of literature supports the presence of microorganisms thriving in the atmosphere associated with aerosols (Gidlen, 1948, Ariya and Amyot, 2004), in snow (Carpenter et al., 2000, Amato et al., 2006) and sea ice (Junge et al., 2002). It is therefore likely that at the snow/sea ice interface, some particles may be of biological origin. Our own bacterial counts showed that bacterial cells were present at concentrations between 10^4 and 10^5 cells mL^{-1} in snow over sea ice or over lake ice (Table 3). These concentrations are in good agreement with previously published numbers for European Arctic snow (Amato et al., 2006). Junge et al. (2004) showed that active bacteria are mostly associated with particles in both melted and intact sea ice. This juxtaposition of particulate Hg and bacterial cells suggests that interactions between Hg and polar microorganisms merit further investigation. This biological activity could potentially produce extracellular biogenic sulphur-containing compounds. Such moieties, released into the dissolved phase during snowmelt and exhibiting a very high affinity for mercury (Stumm and Morgan, 1996), could play an important role in the Hg cycle.

Table 3
Physico-chemical variables of the transect and depth snow profiles carried out on Cornwallis Island

Site	pH	Bacterial counts (cell ml^{-1})	Cl^- (μmol L^{-1})	Br^- (μmol L^{-1})	NO_3^- (μmol L^{-1})	SO_4^{2-} (μmol L^{-1})
Fresh snow (26-JUN-04)	6.0	1.20×10^5	6.34	<d.l.	5.21	0.56
Coastal site surface stratum (S1)[a]	9.0	5.17×10^5	267	0.493	2.36	14.0
Coastal middle stratum (S2)[a]	9.0	1.31×10^5	3.62×10^3	6.00	5.29	145.0
Coastal bottom stratum (S3)[a]	8.5	1.58×10^5	1.657×10^5	116.5	<d.l.	2.699×10^4
Inland site surface	8.4	1.45×10^5	6.16	<d.l.	6.33	0.43
Inland intermediate stratum 1	8.4	4.46×10^5	42.6	<d.l.	6.10	2.64
Inland intermediate stratum 2	8.1	2.01×10^5	76.6	<d.l.	8.08	3.25
Inland site bottom	8.3	2.09×10^5	41.2	<d.l.	5.47	3.20
Transect 1	7.2	1.81×10^5	164	0.255	3.23	1.39
Transect 2	7.0	1.40×10^5	17.8	<d.l.	<d.l.	<d.l.
Transect 3	6.7	2.70×10^5	8.71	<d.l.	2.79	<d.l.
Transect 4	6.4	1.42×10^5	14.6	<d.l.	1.74	0.792
Transect 5	5.8	1.03×10^5	10.1	<d.l.	3.38	6.08
Transect 6	5.6	8.71×10^4	14.9	<d.l.	5.71	3.55
Transect 7	5.5	1.56×10^5	10.3	<d.l.	2.66	0.717
Transect 8	5.0	1.44×10^5	12.4	<d.l.	1.64	3.80
Transect 9	7.0	7.24×10^4	18.0	<d.l.	1.27	<d.l.
Transect 10	6.5	1.94×10^5	326	0.783	3.14	1.91
Transect 11	6.0	2.65×10^5	308	<d.l.	<d.l.	<d.l.

[a] Refers to the snow strata observed over sea ice.

4.2. Accumulation of [THg] at the snow/ice interface

Over sea-ice, [THg] increased with depth and was strongly correlated with concentrations of halides such as chloride or bromide, which are proxies for reactive halogen radicals known to be involved in mercury depletion events (Ariya et al., 2002, Raofie and Ariya, 2004). The increase of [THg] observed at the bottom of the snowpack at the sea ice/snow interface (Fig. 4a) may result from (i) infiltration into the snowpack of underlying water with high [THg]; (ii) increases of [THg] due to the salt enrichment effect observed during sea ice formation (Thomas and Papadimitriou, 2003); or (iii) enrichment from atmospheric origin. The very high concentrations recorded at the snow/sea ice interface may initially originate form atmospheric deposition and subsequent redistribution of Hg species, for the following reasons. First, upward infiltration of underlying water cannot explain high [Hg] at the snow/ice interface, since total Hg concentrations in seawater in this area were the lowest that we observed (1.1–3.8 pmol L^{-1}). The salt enrichment effect is also unlikely. Indeed, assuming that dissolved Hg in seawater is mostly present in the form of negatively charged chlorocomplexes (HgCl42-), based on [Cl$^-$] and [THg] encountered in the area, and assuming a conservative behaviour for Hg and Cl$^-$ upon freezing, we would expect the Cl/Hg ratio to be conserved. The Cl/Hg ratio in seawater was ca. 10^8, whereas it was much lower (10^3) at the sea ice/snow interface; therefore, an alternative source of Hg was likely involved.

Douglas et al. (2005) showed that crystals that form from the vapour phase in direct proximity to open water areas such as leads, exhibited Hg concentrations reaching ca. 4 nmol L^{-1}, which are almost an order of magnitude higher than any reported concentrations in snow in the Arctic (Lu et al., 2001, Lindberg et al., 2002). The authors proposed that frost flowers and surface hoar crystals developing near the leads may be efficient scavengers of atmospheric oxidized Hg species due to their large specific surface areas, therefore increasing [THg]. Although this process certainly contributes to an increase of [THg] in Arctic marine environments, it is unlikely to explain the observed pattern here since (i) we sampled the bottom stratum of the snow accumulation, a layer not directly exposed to air and less subject to deposition of vapour crystals and (ii) large open water bodies were not present in proximity to our sampling site. Note that we sampled ca. 100 m from a crack in sea ice which was 10–50 cm wide. Open water was present ca. 40 km southwest of the sampling site (Fig. 1. area with a white triangle, data from Regional Ice Analysis, Eastern Arctic, Canadian Ice service, Environment Canada, 2004). Note that since these crystals may be involved in mercury depletion events and that they are likely incorporated to the sea ice matrix, some areas within sea ice may be enriched with Hg. Because of the heterogeneity of sea ice, a transfer of Hg from these areas to the overlying snow, remains to be determined.

Finally, Hg could have been redistributed, possibly associated with particles, after its deposition as a result of alteration of the physical properties of snow influenced by environmental factors (e.g. wind, temperature gradient and humidity) both during cold conditions (dry snow metamorphism) and during the melting period (wet snow metamorphism). Although the bottom layer where Hg had accumulated showed few signs of destructive metamorphism, sampling occurred after the surface temperature exceeded 0 °C for the first time, and therefore the possible infiltration of melt waters cannot be ruled out (note that we did observe some ice lenses within the accumulation). Seasonal snowpacks are heterogeneous, especially on a short spatial scale (ca. 10 m) due to wind, water percolation and topography (Sturm and Benson, 2004) and the actual physical snow properties observed on this date may vary over greater scale.

That both dry and wet snow metamorphism may influence the redistribution of Hg species is supported by the following reasons. First, it has been shown in previous studies that ionic species behave very differently from one another with respect to their elution sequence from the snowpack. Cragin et al. (1996) concluded that fractionation and preferential elution were strongly influenced by ion exclusion and rearrangement processes occurring during dry snow metamorphism, independent of the melt-freeze cycle. Although this latter study mostly focused on anionic species, it may be a starting point to better understand the behaviour of a cationic species such as mercury, especially since it was shown that snow does not exhibit chromatographic properties (Cragin et al., 1996, Eichler et al., 2001) and should therefore not discriminate among species on the basis of their charge. Rather, the authors argue that the elution sequence is likely controlled by the initial position of the ion in the original snow crystal—i.e. as part of the nuclei or adsorbed at the surface—which is dependent on snow formation and scavenging processes in the atmosphere. Second, it is likely that processes that drive movement of particulate Hg within the snow accumulation differ from those that affect the migration of dissolved species. The work by Conway et al. (1996) suggests that particles smaller than 5 μm (e.g. soot or ash) are more mobile than those of greater size which are virtually immobile until actual massive melt occur. It is common to observe percolation columns of meltwaters, especially during the melting period (Jones et al., 2001), which bridge the upper and bottom parts of the snow accumulation. These columns may be responsible for the transfer of mercury species deposited at the surface, towards the bottom the accumulation.

4.3. Impact of melting inland and marine snowpacks on underlying waters

Depth profiles carried out in the water column of the lake and the upper part of the seawater column showed that THg concentrations were 3–4 times greater at the surface than deeper in the water column. This is most likely due to the presence of the melting snowpack which sits on top of the ice. The presence of a greater proportion of Hg bound to particles at the surface of seawater, between sea ice edges, than at depths of 5.5 and 11.5 m, also suggests an influence of the snowpack since most of the Hg present in snow is bound to particles (see above). Note also that when considering all measured cationic elements, only Hg exhibited concentrations higher in snow than in the underlying water (Snow/Sea Hg ratio >79; see last line of Table 4 and Fig. 5b). This represents the first evidence that a melting snowpack contributes to increasing THg concentrations at the sea ice/water interface. Combined these results suggest that even though an important fraction of the Hg deposited during mercury depletion events may be reemitted back to the atmosphere, the interface between sea ice and snow constitutes a build-up site for particulate Hg species increasing [THg] in surface water.

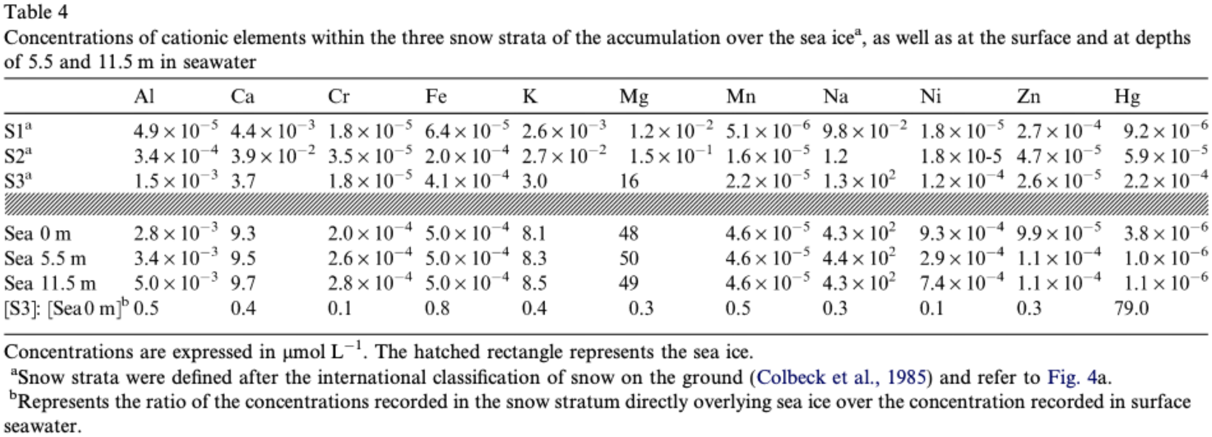

Table 4

Concentrations of cationic elements within the three snow strata of the accumulation over the sea ice[a], as well as at the surface and at depths of 5.5 and 11.5 m in seawater

	Al	Ca	Cr	Fe	K	Mg	Mn	Na	Ni	Zn	Hg
S1[a]	4.9×10^{-5}	4.4×10^{-3}	1.8×10^{-5}	6.4×10^{-5}	2.6×10^{-3}	1.2×10^{-2}	5.1×10^{-6}	9.8×10^{-2}	1.8×10^{-5}	2.7×10^{-4}	9.2×10^{-6}
S2[a]	3.4×10^{-4}	3.9×10^{-2}	3.5×10^{-5}	2.0×10^{-4}	2.7×10^{-2}	1.5×10^{-1}	1.6×10^{-5}	1.2	$1.8\times$10-5	4.7×10^{-5}	5.9×10^{-5}
S3[a]	1.5×10^{-3}	3.7	1.8×10^{-5}	4.1×10^{-4}	3.0	16	2.2×10^{-5}	1.3×10^{2}	1.2×10^{-4}	2.6×10^{-5}	2.2×10^{-4}
▨	▨	▨	▨	▨	▨	▨	▨	▨	▨	▨	▨
Sea 0 m	2.8×10^{-3}	9.3	2.0×10^{-4}	5.0×10^{-4}	8.1	48	4.6×10^{-5}	4.3×10^{2}	9.3×10^{-4}	9.9×10^{-5}	3.8×10^{-6}
Sea 5.5 m	3.4×10^{-3}	9.5	2.6×10^{-4}	5.0×10^{-4}	8.3	50	4.6×10^{-5}	4.4×10^{2}	2.9×10^{-4}	1.1×10^{-4}	1.0×10^{-6}
Sea 11.5 m	5.0×10^{-3}	9.7	2.8×10^{-4}	5.0×10^{-4}	8.5	49	4.6×10^{-5}	4.3×10^{2}	7.4×10^{-4}	1.1×10^{-4}	1.1×10^{-6}
[S3]: [Sea 0 m][b]	0.5	0.4	0.1	0.8	0.4	0.3	0.5	0.3	0.1	0.3	79.0

Concentrations are expressed in μmol L^{-1}. The hatched rectangle represents the sea ice.

[a] Snow strata were defined after the international classification of snow on the ground (Colbeck et al., 1985) and refer to Fig. 4a.

[b] Represents the ratio of the concentrations recorded in the snow stratum directly overlying sea ice over the concentration recorded in surface seawater.

4.4. Conceptual summary

Conceptual representations of Hg dynamics and distribution in an Arctic snowpack from early spring to summer, summarizing the main conclusions of this paper, are presented in Fig. 7a and b. Inland sites can experience enhanced mercury deposition due to winds (Fig. 7a (1) and (2)), which carry the products of the fast oxidation of gaseous elemental mercury occurring in coastal/marine environments (Fig. 7b (1)). A growing body of literature shows that mercury depletion events are transitory and when light conditions are optimal, part of the Hg deposited onto snow surface is efficiently recycled back to the atmosphere within days, therefore limiting the impact of deposition to aquatic systems. However, because of enhanced oxidative processes occurring in the marine environment, the photoreduction of Hg(II) and subsequent evasion of the newly produced Hg(0) are hampered, and hence marine environments tend to accumulate more Hg than inland sites (Fig. 7a (3) and Fig. 7b (2)). At the onset of snowmelt, Hg was mostly bound to particles, especially over sea-ice. This observation probably reflects both the impact of particle-associated reactions that led to Hg deposition and the subsequent redistribution due to water phase changes. Here, the snow/sea ice interface was identified as a location where Hg accumulates (Fig. 7b (3)), reaching concentrations one order of magnitude greater than what is observed at the surface or at inland sites, where no such accumulation was observed (Fig. 7a (4)). The mechanisms of Hg transport are still unclear but may involve changes in snow physical properties related to metamorphism. During snowmelt, the presence of percolation columns may also affect downward Hg transport. Another as yet totally unknown aspect of Hg cycling in polar areas is Hg dynamics within the heterogeneous matrix of sea ice and namely whether transport and transformation of Hg occur within sea ice (Fig. 7a; (4)). As snow melts, a significant fraction of Hg is exported to aquatic systems, resulting in significant increases in [THg] at the top of the water columns, both at inland (Fig. 7a (5)) and coastal sites (Fig. 7b (5)). The impact of melting snow packs on underlying seawater (Fig. 7a and b; (6)), where dense populations of sea ice algae thrive (Mundy et al., 2005), may constitute an important link between arctic Hg cycling and biota contamination.

Acknowledgments

We gratefully acknowledge funding from the Canadian Foundation for Climate and Atmospheric Science (CFCAS), the Natural Sciences and Engineering Research Council of Canada (NSERC) and the Collaborative Mercury Research Network (COMERN) to M.A. and P.A.A. as well as the Science Horizon program to M.A. We would like to thank Dr. T. Douglas for his insightful comments as well as the editor and two other reviewers who contributed to greatly improve this manuscript. We thank B.E. Keatley for her comments on the manuscript. We also would like to thank the Polar Continental Shelf Project for their logistic support to M.A. as well as the Nunavut Research Institute that

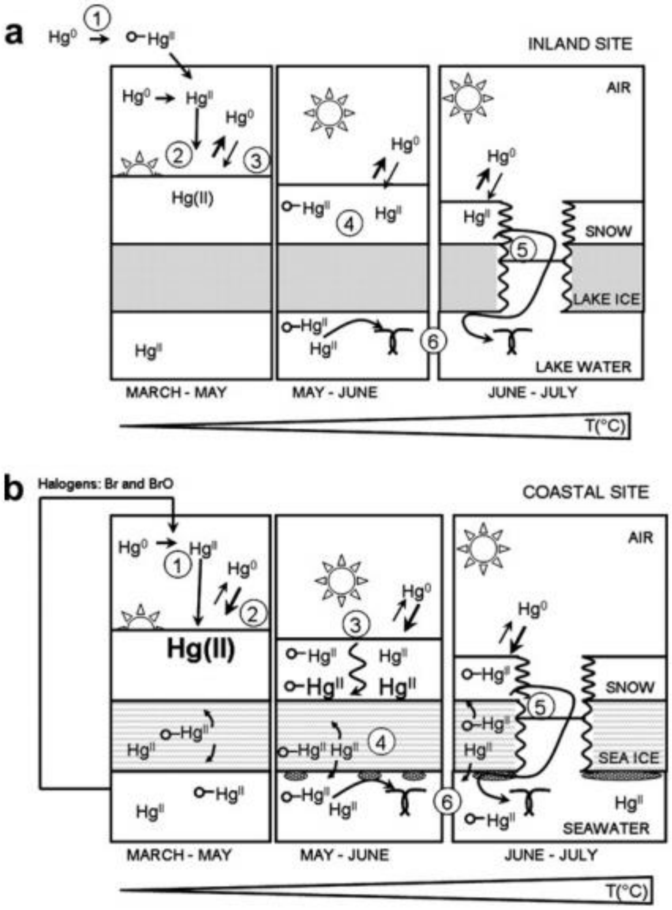

Fig. 7. Schematic summary of Hg dynamics at the air/snow/ice/water interfaces in a polar environment (a) over lake ice and (b) over sea ice. Numbers refer to the text of Section 4.4. conceptual summary. Note the height of the sun is related to its energy over the period of time depicted in the scheme.

period (Jones et al., 2001), which bridge the upper and bottom parts of the snow accumulation. These columns may be responsible for the transfer of mercury species deposited at the surface, towards the bottom the accumulation.

delivered our research license. We express our gratitude to Dr. Paul del Giorgio at UQAM for access to the flow cytometer and to Dr. H. Vali for access to the electron microscopy facility at McGill University. We would like to warmly thank Paddy Aqiatusuk as well as Debbie Iqaluk for their outstanding help and support in the field, Louise Pelletier, for her help with the electron microscope at the University de Montréal and Dominic Belanger for his help in the lab. This is contribution PCSP# 020-07.

References

Amato P., Hennebelle R., Magand O., Sancelme M., Delort A.-M., Barbante C., Boutron C., and Ferrari C. (2006) Bacterial characterization of the snowcoverat Spitzberg, Svalbard. FEMS Microbiol. Ecol. 59(2), 255–264.

Ariya P. A., and Amyot M. (2004) New directions: the role of bioaerosols in atmospheric chemistry and physics. Atmos. Environ. 38(8), 1231–1232.

Ariya P. A., Dastoor A. P., Amyot M., Schroeder W. H., Barrie L., Anlauf K., Raofie F., Ryzhkov A., Davignon D., Lalonde J., and Steffen A. (2004) The Arctic: a sink for mercury. Tellus Ser. B-Chem. Phys. Meteorol. 56(5), 397–403.

Ariya P. A., Khalizov A., and Gidas A. (2002) Reactions of gaseous mercury with atomic and molecular halogens: kinetics, product studies, and atmospheric implications. J. Phys. Chem. A 106(32), 7310–7320.

Carpenter E. J., Lin S. J., and Capone D. G. (2000) Bacterial activity in South Pole snow. Appl. Environ. Microbiol. 66(10), 4514–4517.

Colbeck S., Akitaya E., Armstrong R., Gubler H., Lafeuille J., Lied K., McClung D., and Morris E. (1985) The International Commission on Snow and Ice of the International Association of Scientific Hydrology and the International Glaciological Society.

Conway H., Gades A., and Raymond C. F. (1996) Albedo of dirty snow during conditions of melt. Water Resour. Res. 32(6), 1713–1718.

Cragin J. H., Hewitt A. D., and Colbeck S. C. (1996) Grain-scale mechanisms influencing the elution of ions from snow. Atmos. Environ. 30(1), 119–127.

Dommergue A., Ferrari C. P., Gauchard P. A., Boutron C. F., Poissant L., Pilote M., Jitaru P., and Adams F. C. (2003a). The fate of mercury species in a sub-arctic snowpack during snowmelt. Geophys. Res. Lett. 30 (12 Art. No. 1621).

Dommergue A., Ferrari C. P., Poissant L., Gauchard P. A., and Boutron C. F. (2003b) Diurnal cycles of gaseous mercury within the snowpack at Kuujjuarapik/Whapmagoostui, Quebec, Canada. Environ. Sci. Technol. 37(15), 3289–3297.

Douglas T. A., and Sturm M. (2004) Arctic Haze, mercury and the chemical composition of snow across northwestern Alaska. Atmos. Environ. 38(6), 805–820.

Douglas T. A., Sturm M., Simpson W. R., Brooks S., Lindberg S. E., and Perovich D. K. (2005) Elevated mercury measured in snow and frost flowers near Arctic sea ice leads. Geophys. Res. Lett. 32(4).

Ebinghaus R., Kock H. H., Temme C., Einax J. W., Lowe A. G., Richter A., Burrows J. P., and Schroeder W. H. (2002) Antarctic springtime depletion of atmospheric mercury. Environ. Sci. Technol. 36(6), 1238–1244.

Eichler A., Schwikowski M., and Gaggeler H. W. (2001) Meltwater-induced relocation of chemical species in Alpine firn. Tellus Ser. B-Chem. Phys. Meteorol. 53(2), 192–203.

Ferrari C. P., Dommergue A., Boutron C., Jitaru P., and Adams F. C. (2004) Profiles of Mercury in the snow pack at Station Nord, Greenland, shortly after polar sunrise. Geophys. Res. Lett. 31, L03401.

Ferrari C. P., Dommergue A., Veysseyre A., Planchon F., and Boutron C. F. (2002) Mercury speciation in the French seasonal snow cover. Sci. Total Environ. 287(1–2), 61–69.

Gasol J. M., and Del Giorgio P. A. (2000) Using flow cytometry for counting natural planktonic bacteria and understanding the structure of planktonic bacterial communities. Scientia Marina 64(2), 197–224.

Gauchard P. A., Ferrari C. P., Dommergue A., Poissant L., Pilote M., Guehenneux G., Boutron C. F., and Baussand P. (2005) Atmospheric particle evolution during a nighttime atmospheric mercury depletion event in sub-arctic at kuujjuarapik/ Whapmagoostui, Quebec, Canada. Sci. Total Environ. 336, 215–224.

Gidlen T. (1948) Aerial plankton and its conditions of life. Biol. Rev. 23, 109–126.

Gill G. A., and Bruland K. W. (1990) Mercury speciation in surface fresh-water systems in California and other areas. Environ. Sci. Technol. 24(9), 1392–1400.

Jones G. H., Pomeroy J. W., Walker D. A., and Hoham R. W. (2001) Snow Ecology: An Interdisciplinary Examination of Snow-Covered Ecosystems. Cambridge University Press.

Junge K., Eicken H., and Deming J. W. (2004) Bacterial activity at 2 to 20

C in Arctic wintertime sea ice. Appl. Environ. Microbiol. 70(1), 550–557.

Junge K., Imhoff F., Staley T., and Deming J. W. (2002) Phylogenetic diversity of numerically important arctic sea-ice bacteria cultured at subzero temperature. Microbial Ecol. 43(3), 315–328.

Lalonde J. D., Amyot M., Doyon M. R., and Auclair J. C. (2003) Photo-induced Hg(II) reduction in snow from the remote and temperate Experimental Lakes Area (Ontario, Canada). J. Geophys. Res. -Atmos. 108(D6).

Lalonde J. D., Amyot M., Kraepiel A. M. L., and Morel F. M. M. (2001) Photooxidation of Hg(0) in artificial and natural waters. Environ. Sci. Technol. 35(7), 1367–1372.

Lalonde J. D., Poulain A. J., and Amyot M. (2002) The role of mercury redox reactions in snow on snow-to-air mercury transfer. Environ. Sci. Technol. 36(2), 174–178.

Lindberg S. E., Brooks S., Lin C. J., Scott K. J., Landis M. S., Stevens R. K., Goodsite M., and Richter A. (2002) Dynamic oxidation of gaseous mercury in the Arctic troposphere at polar sunrise. Environ. Sci. Technol. 36(6), 1245–1256.

Lu J. Y., and Schroeder W. H. (2004) Annual time-series of total filterable atmospheric mercury concentrations in the Arctic. Tellus Ser. B-Chem. Phys. Meteorol. 56(3), 213–222.

Lu J. Y., Schroeder W. H., Barrie L. A., Steffen A., Welch H. E., Martin K., Lockhart L., Hunt R. V., Boila G., and Richter A. (2001) Magnification of atmospheric mercury deposition to polar regions in springtime: the link to tropospheric ozone depletion chemistry. Geophys. Res. Lett. 28(17), 3219–3222.

Mundy C. J., Barber D. G., and Michel C. (2005) Variability of snow and ice thermal, physical and optical properties pertinent to sea ice algae biomass during spring. J. Mar. Syst. 58(3–4), 107–120.

Poissant L., and Pilote M. (2003) Time series analysis of atmospheric mercury in Kuujjuarapik/Whapmagoostui (Quebec). J. Phys. IV 107, 1079–1082.

Poulain A. J., Lalonde J. D., Amyot M., Shead J. A., Raofie F., and Ariya P. A. (2004) Redox transformations of mercury in an Arctic snowpack at springtime. Atmos. Environ. 38(39), 6763– 6774.

Raofie F., and Ariya P. A. (2004) Product study of the gas-phase BrO-initiated oxidation of Hg-0: evidence for stable Hg1+ compounds. Environ. Sci. Technol. 38(16), 4319–4326.

Riordan E., Minogue N., Healy D., O'Driscoll P., and Sodeau J. R. (2005) Spectroscopic and optimization modeling study of nitrous acid in aqueous solution. J. Phys. Chem. A 109(5), 779–786.

Ritchie C. D., Richards W., and Arp P. A. (2006) Mercury in fog on the Bay of Fundy (Canada). Atmos. Environ. 40(33), 6321– 6328.

Sarica J., Amyot M., and Hare L. (2004) An easy method to measure total particulate Hg in water without chemical digestion. Water Air and Soil Poll. 151(1–4), 3–10.

Schecher W. D., and McAvoy D. C. (1992) Mineql+—a software environment for chemical-equilibrium modeling. Comput. Environ. Urban Syst. 16(1), 65–76. Schroeder W. H., Anlauf K. G., Barrie L. A., Lu J. Y., Steffen A., Schneeberger D. R., and Berg T. (1998) Arctic springtime depletion of mercury. Nature 394(6691), 331–332.

Sprovieri F., Pirrone N., Landis M. S., and Stevens R. K. (2005) Oxidation of gaseous elemental mercury to gaseous divalent mercury during 2003 polar sunrise at Ny-Alesund. Environ. Sci. Technol. 39(23), 9156–9165.

St Louis V. L., Sharp M. J., Steffen A., May A., Barker J., Kirk J. L., Kelly D. J., Arnott S. E., Keatley B., and Smol J. P. (2005) Some sources and sinks of monomethyl and inorganic mercury on Ellesmere Island in the Canadian High Arctic. Environ. Sci. Technol. 39(8), 2686–2701.

Staebler R. M., Denhartog G., Georgi B., and Dusterdiek T. (1994) Aerosol-size distributions in Arctic Haze during the polar sunrise experiment 1992. J. Geophys. Res.-Atmos. 99(D12), 25429– 25437.

Steffen A., Schroeder W., Bottenheim J., Narayan J., and Fuentes J. D. (2002) Atmospheric mercury concentrations: measurements and profiles near snow and ice surfaces in the Canadian Arctic during Alert 2000. Atmos. Environ. 36(15–16), 2653– 2661.

Stumm W. and Morgan J. J. (1996) Metal ions in aqueous solution: aspects of coordination chemistry. In Aquatic Chemistry— Chemical Equilibria and Rates in Natural Waters, third ed. (eds. J. L. Schnoor, and A. Zehnder), Wiley, p. 1022.

Sturm M., and Benson C. (2004) Scales of spatial heterogeneity for perennial and seasonal snow layers. In Annals of Glaciology, vol. 38, pp. 253–260.

Swain E. B., Engstrom D. R., Brigham M. E., Henning T. A., and Brezonik P. L. (1992) Increasing rates of atmospheric mercury deposition in midcontinental North-America. Science, 784–787.

Thomas D. N. and Papadimitriou S. (2003) Biogeochemistry of sea ice. In Sea Ice: An Introduction to its Physics, Chemistry, Biology and Geology (eds. D. N. Thomas and G. S. Dieckmann), Blackwell Science Ltd., pp. 267–302

Toom-Sauntry D., and Barrie L. A. (2002) Chemical composition of snowfall in the high Arctic: 1990–1994. Atmos. Environ. 36(15–16), 2683–2693.

Vogt R., Crutzen P. J., and Sander R. (1996) A mechanism for halogen release from sea-salt aerosol in the remote marine boundary layer. Nature 383, 327–330.

Weathers K. C. (1999) The importance of cloud and fog in the maintenance of ecosystems. Trends Ecol. Evol. 14(6), 214–215.